J. Eng. Technol. Sci., Vol. 53, No. 6, 2021, 210613

Experimental Work for Bar Straightness Effect Evaluation of Split Hopkinson Pressure Bar

Afdhal, Leonardo Gunawan*, Tatacipta Dirgantara & Sigit Puji Santosa

Lightweight Structures Research Group, Faculty of Mechanical and Aerospace Engineering, Institut Teknologi Bandung,
Jalan Ganesa No. 10 Bandung 40132, Indonesia
*E-mail: gun@ftmd.itb.ac.id

Highlights:

- This work contributes to the development of experimental study by validating a numerical model of the Split Hopkinson Pressure Bar regarding the straightness effect of the bar components.
- Experimental work was conducted on two kinds of materials, i.e. ST37 and aluminum 6061. The results showed that the current bar straightness condition of the SHPB tested did not significantly affect the strain wave signal.
- Good agreement between the experimental results and the numerical simulation results was obtained in terms of strain rates and the stress-strain relationship.
- This work suggests a new recommendation for bar straightness tolerance that is more applicable. The recommended bar straightness tolerance is proposed as 0.36 mm per 100 mm.

Abstract. Bar straightness is one of several factors that can affect the quality of the strain wave signal in a Split Hopkinson Pressure Bar (SHPB). Recently, it was found that the bar components of the SHPB at the Lightweight Structures Laboratory displayed a deviation in straightness because of manufacturing limitations. An evaluation was needed to determine whether the strain wave signals produced from this SHPB are acceptable or not. A numerical model was developed to investigate this effect. In this paper, experimental work was performed to evaluate the quality of the signal in the SHPB and to validate the numerical model. Good agreement between the experimental results and the numerical results was obtained for the strain rates and stress-strain relationship for mild steel ST37 and aluminum 6061 specimen materials. The recommended bar straightness tolerance is proposed as 0.36 mm per 100 mm.

Keywords: *aluminum 6061; bar straightness; experimental work; mild steel; SHPB.*

1 Introduction

Investigation of the high strain rate properties of materials is among the most instrumental research areas for safety-critical applications. Several techniques have been developed through various researches to obtain these properties. John Hopkinson conducted the seminal experiment that was the foundation for the measurement of high strain rate material properties: an investigation into the

Received April 13th, 2021, Revised May 10th, 2021, Accepted for publication May 21st, 2021.
 ISSN: 2337-5779,
DOI: 10.5614/j.eng.technol.sci.2021.53.6.13

rupture of an iron wire under a blow by a moving mass led to the critical conclusion that a stress wave propagates along the wire [1-2]. More research on this topic was done until Kolsky in 1949 proposed an extension of the Hopkinson bar technique for the dynamic characterization of materials. He proposed to use two elastic bars with one specimen sandwiched in between [3]. This technique is used until today and is known as the Split Hopkinson Pressure Bar or Kolsky bar to honor his idea.

The need to acquire the mechanical properties of various materials at high strain rates has increased over the years. Studies have been reported on the high strain rate properties of various materials such as steel [4-7], aluminum foam [8-11], composite [12-18], polymer [19-26], and ceramic [27-28]. Delving deeper into SHPB experimental works, the issue of signal quality recorded by the strain gauges attached to the bar components has been studied by several researchers. This issue is not only related to the data acquisition system but also to the standard and the desired tolerance of the SHPB components, which may affect the validity of SHPB experimental work. There are a number of factors that may affect the quality of the strain wave signals from an SHPB, one of which is bar straightness [29-30]. The bars of the SHPB in the Lightweight Structures Laboratory at FMAE ITB were recently found to have a deviation of straightness caused by manufacturing limitations. An evaluation was needed to determine whether the strain wave signals produced by this SHPB are acceptable or not. A numerical model was developed to address this issue, which indicated that the signal quality produced by this SHPB is still acceptable [31]. In the present study, experimental work was done to confirm the results obtained from the numerical simulation. The contribution of this work is to propose a refined correction of the bar straightness tolerance that has previously been proposed by other researchers, i.e. Kariem, *et al.* [29] and Song, *et al.* [32]. Two types of specimen materials were used: mild steel ST37 and aluminum 6061. The specimens were manufactured as solid cylinders. Comparison between the experimental and the numerical results was conducted to evaluate the quality of the strain wave signals.

2 Theoretical Background

The SHPB is an instrument that is widely used to obtain the mechanical properties of materials at high strain rates 500-10^4/s [33-36]. The relationship between the stress and strain in a material in the form of a stress-strain curve can be obtained using an SHPB. One-dimensional stress wave theory is used for the calculation of strains, stresses, and strain rates for SHPBs [37]. Equations (1)-(3) are the formulas to calculate strain rates, strains, and stresses for SHPBs, respectively [38]. The assumptions of this theory are that the bar system must be linear and dispersion-free. This assumption requires the SHPB system to comply with several criteria, including having a uniform cross section area, remaining linear elastic during the test, staying homogenous and isotropic, and having a straight neutral axis – a pre-requisite for bar straightness as the focus of this paper [39-41].

$$\dot{\varepsilon}(t) = -\frac{2c_0}{L_s}\varepsilon_R(t) \tag{1}$$

$$\varepsilon(t) = -\frac{2c_0}{L_s}\int_0^t \varepsilon_R(t)dt \tag{2}$$

$$\sigma(t) = \frac{AE}{A_s}\varepsilon_T(t) \tag{3}$$

The bar system in the SHPB is arranged from three different bars: striker bar, incident bar, and transmitter bar, positioned on a one-line neutral axis, as illustrated in Figure 1. The specimen is sandwiched between the incident bar and the transmitter bar.

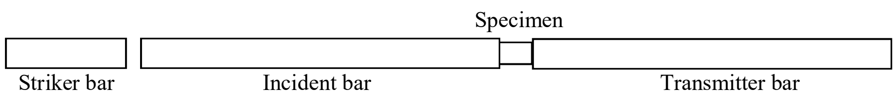

Figure 1 SHPB schematic drawing.

The striker bar as loading generator is moved by high-pressure nitrogen gas released from a high-pressure tank. This bar impacts the incident bar so that an incident strain wave in the form of a compressive wave is generated and propagated along the incident bar. At the interface of the incident bar and the specimen, part of this wave will be reflected as a tensile strain wave and another wave is transmitted as a compressive strain wave propagating through the specimen and the transmitter bar. The reflected wave and the transmitted strain wave are used in the calculation of strain rates, strains, and stresses measured by an SHPB [41]. A typical SHPB strain wave signal is shown in Figure 2.

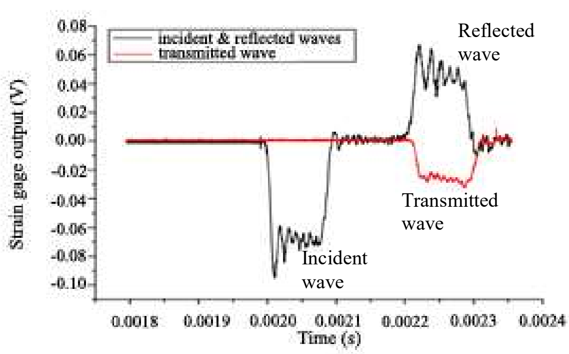

Figure 2 Typical SHPB strain wave signal from experimental work [36].

3 Experimental Set-up

Experimental work was conducted using an SHPB system in the Lightweight Structures Laboratory, as shown in the 3. The bars are made from AISI 4340 with a diameter of 10 mm and a length of 1000 mm. The deviation data of bar straightness refers to a previous publication on the numerical model of this case study, as summarized in Table 1 [31]. The deflection of the bar in the y-direction was measured using dial gauges by dividing it into 10 sections and setting every final position of the previous section to zero.

Strain gauges with a resistance of 120 Ohm and data acquisition with a frequency response of 103 kHz were used in this experiment to record the strain wave signal during the tests. Aluminum 6061 and mild steel ST37 were used as specimen materials. A cylindrical shape with a radius and thickness of 8 mm and 8 mm respectively was chosen. Experimental tests using these specimens were performed using 85 psi pressure, which is equivalent to a striker velocity of 20 m/s.

As the initial step in the SHPB experimental work, the striker bar velocity was measured using a speed sensor for every pressure given to move the bar. The relationship curve between speed and pressure was then constructed as shown in Figure 3. This curve is important because it can be used to predict the magnitude of the striker bar velocity that can be generated from a given pressure. The striker bar velocity is usually used as an input parameter in numerical simulations.

Two calibration procedures were conducted at the beginning of the experimental work using 85 psi pressure (20 m/s). A bar apart test involving the striker and the incident bar was conducted to calibrate the quality of the strain wave signal in the incident bar. In the bar apart test, a compressive strain wave signal is generated by the incident bar impacting the striker bar. This signal then propagates along the incident bar and reflects when it reaches the end of the bar. Comparison between the incident strain wave and the reflected strain wave is conducted to evaluate the quality of the signals inside the incident bar to assess the bar straightness effect. A combined bar test procedure involving the striker bar, the incident bar, and the transmitter bar is subsequently performed to evaluate the quality of the strain wave signals in the incident and the transmitter bar. In this procedure, the striker bar will generate a compressive strain wave inside the incident bar and this wave will propagate and transmit to the transmitter bar. Comparison between the compressive strain waves inside the incident and the transmitter bar is performed to evaluate the quality of the signals to assess the bar straightness and alignment.

In this experimental work, bar interface parallelism was controlled so that the contact between striker bar, incident bar, specimen, and transmitter bar could be properly maintained. The specimens were mounted using petroleum jelly between the incident bar and the transmitter bar.

Figure 3 The SHPB in the Lightweight Structure Laboratory at ITB [31].

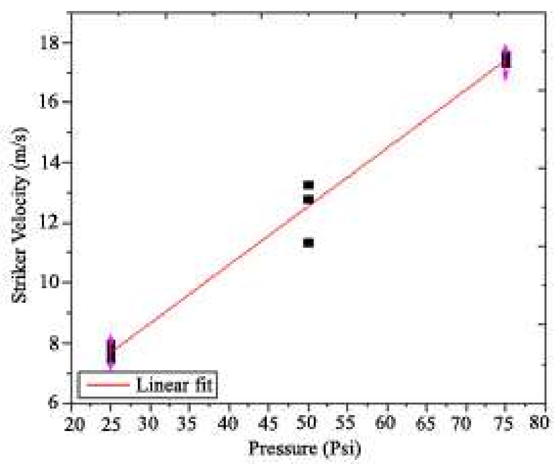

Figure 4 Pressure vs striker bar velocity in linear fit.

Table 1 Bar straightness deviation data [31].

Incident bar y-deviation (mm)									
1	**2**	**3**	**4**	**5**	**6**	**7**	**8**	**9**	**10**
0.03	0.15	-0.12	-0.44	0.09	0.14	0.54	0.29	-0.37	-0.2
Transmitter bar y-deviation (mm)									
1	**2**	**3**	**4**	**5**	**6**	**7**	**8**	**9**	**10**
0.24	-0.24	-0.24	-0.16	-0.62	-0.32	0.53	0.42	0.06	0.63

4 Results and Discussion

Recent relevant research has attempted to standardize the straightness of SHPBs required to acquire reliable experimental data. Song *et al.* recommended that the straightness tolerance of the SHPB bar components should be 0.05 mm per 305 mm [32]. Kariem, *et al.* suggested tolerances of 0.25 mm per 100 mm for bar straightness and ±0.03° or 0.007 mm for a 12.7-mm bar diameter for the bar surface perpendicular to a neutral axis [29].

All sections in the SHPB as shown in Table 1 exceeded the tolerance for bar straightness from Song, *et al.*'s recommendation. However, referring to Kariem, *et al.* [29], there were some sections of the bar that met their recommended tolerance, while some other sections exceeded it. For the incident bar and the transmitter bar, the average values of straightness deviation based on the data provided in Table 1 were 0.24 mm and 0.35 mm per 100 mm, respectively. The average value for the incident bar met the recommendation, except in relation to the transmitter bar. Furthermore, the highest values of bar straightness deviation in the incident bar and the transmitter bar exceeded the tolerance suggested by Kariem, *et al.* at 0.55 mm and 0.66 mm, respectively. These experimental findings were rationalized using a numerical simulation, which showed that the strain wave signals in both the incident and the transmitter bar was deemed acceptable [31]. In the numerical study, strain wave signals in a non-straight bar were compared to those in a perfectly straight one. The difference between the non-straight and perfectly straight bars was 1.07% based on the ringing-up process.

In this study, experimental work was conducted to validate the numerical results. Validation was performed for the bar calibration process and specimen testing. Figures 5 and 6 show a comparison between the experimental and the numerical results for bar calibration.

In the bar apart test, when a bar is in perfectly straight condition, the reflected strain wave will have the same amplitude and duration as the incident strain wave. Hence, the wave dispersion produced driven by the bar straightness deviation can be evaluated by this test. The experimental results of the bar apart test showed that the incident and reflected strain waves had near consistent amplitude and duration. The experimental results were in line with the numerical results for a strain wave duration of 0.13 ms and an amplitude of 0.002, as shown in Figure 5. Based on this, it can be concluded that the quality of the strain waves propagated in the incident bar was acceptable, because it has a shape that is comparable to the numerical simulation results for a perfectly straight bar. In addition, the dispersion that occurred in the non-straight bar is considered acceptable as the shape between the incident strain wave and the reflected strain wave was not significantly different. The difference in strain amplitude between the incident wave and the reflected wave in a non-straight bar from the experimental results was less than 2%. In terms of strain wave duration, there was no difference between the incident wave and the reflected wave.

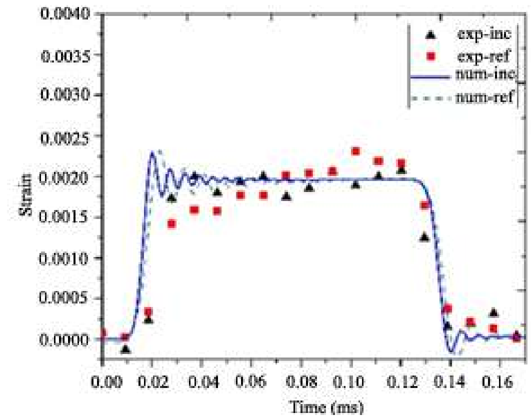

Figure 5 Comparison between experimental and numerical results for bar apart test.

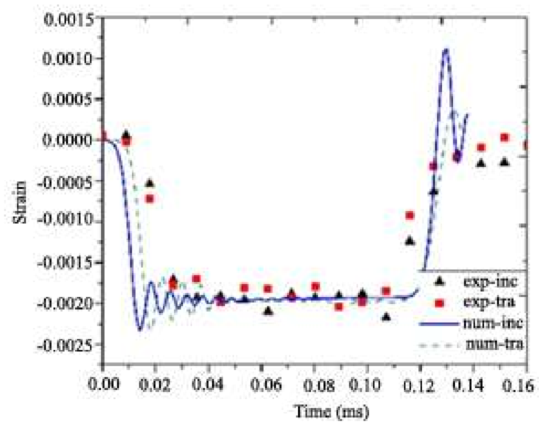

Figure 6 Comparison between experimental and numerical results for combined bar test.

As part of other calibration procedures, a combined bar test was performed to evaluate the quality of the strain wave signal inside the incident bar and the transmitter bar. In an ideal condition, where both the incident bar and the transmitter bar are perfectly straight, the incident strain waves inside the incident bar will have the same shape as the transmitted waves inside the transmitter bar. This is because in a perfectly straight bar the strain waves will propagate in the incident bar and transmit to the transmitter bar with very minimal dispersion. This test is not only useful to evaluate the bar straightness condition but also to evaluate the alignment of the bars in an SHPB. The experimental result for the combined bar test in this study showed that the strain wave signals in the incident bar and the transmitter bar had very good agreement. The amplitude of 0.002 and duration of 0.13 ms of both strain waves were in line as well, as shown in Figure 6 – the experimental results exhibited good agreement with the numerical results. The difference in strain amplitude between the incident wave and the transmitted wave in a non-straight bar for the experimental results was less than 3.5 %. From this result it can be concluded that the strain wave signal quality and bar arrangement in the SHPB is acceptable. Furthermore, for the whole calibration procedure it can be concluded that the experimental work confirmed the rationalized results obtained through the numerical simulation with very good agreement.

Aluminum 6061 and mild steel ST 37 were used as specimen materials in this study. Experimental work was performed with these specimens and compared to the numerical results. Strain rate versus time and stress versus strain were obtained from the experimental work. Figures 7 and 8 show the strain rate results from the experimental work using aluminum 6061 and mild steel ST 37 specimen materials.

The strain rates produced in the SHPB experimental work basically depend on the velocity of the striker bar. A higher strain-rate value for a certain type of specimen material can be obtained by increasing the velocity of the striker bar. In this study, the striker bar speed was set at 20 m/s, produced by 85 psi pressure. The strain rates obtained from the experimental work with aluminum 6061 and mild steel ST37 were 1227/s and 1283/s, respectively. When compared to the numerical results shown in Figure 7 and 8, the experimental results differed by 1.5% for the aluminum 6061 and 1.9% for the mild steel ST37. The strain rates were determined after the ringing-up process described in Figure 7.

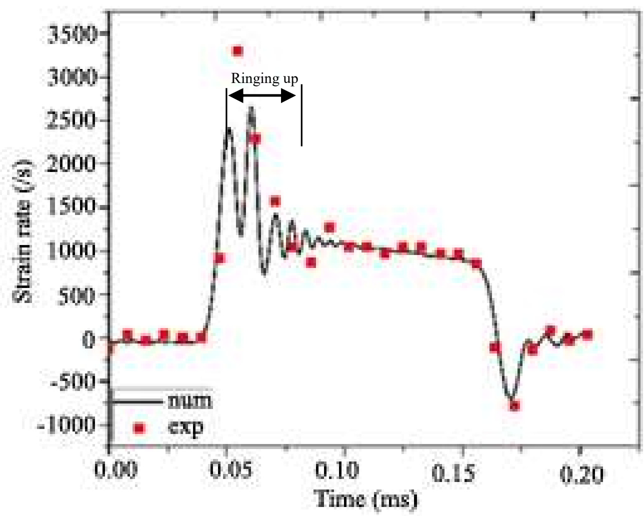

Figure 7 Strain rate curve for aluminum 6061.

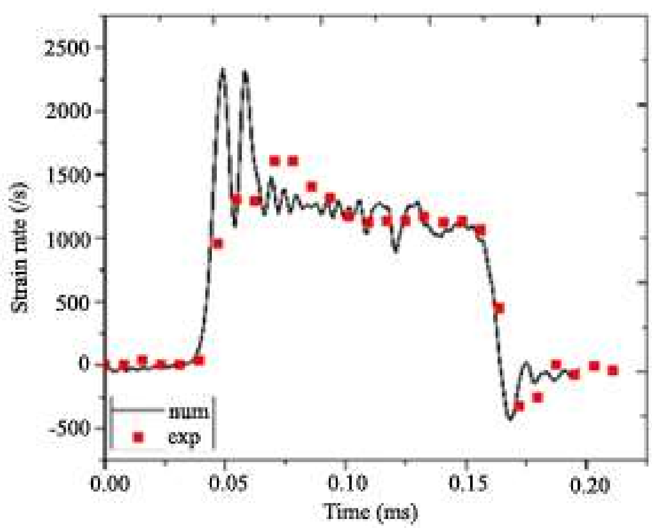

Figure 8 Strain rate curve for mild steel ST37.

The stress-strain curves obtained from the SHPB experimental work are shown in Figures 9 and 10 for the aluminum 6061 and the mild steel ST37, respectively. The stress-strain curves shown only cover the plastic region. The modulus of elasticity in the SHPB experimental work was assumed to be the same as that obtained under static or quasi-static condition [35].

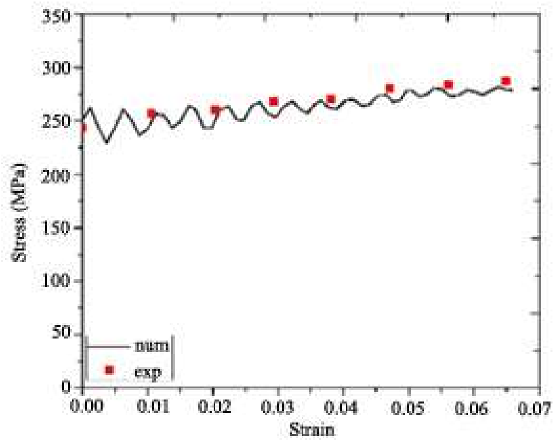

Figure 9 Experimental and numerical comparison for stress-strain curve for the aluminum 6061 specimen material.

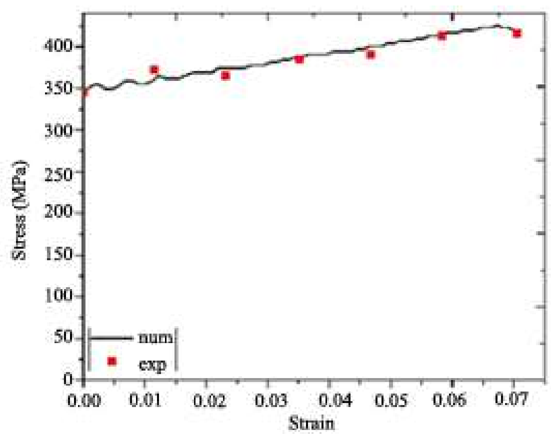

Figure 10 Experimental and numerical comparison for stress-strain curve for the mild steel ST37 specimen.

The experimental stress-strain curve for the aluminum 6061 was very close to the numerical one. The yield stress, i.e. the onset in the graph, obtained experimentally was 244 MPa, or 3% lower than from the numerical result. However, the experimental flow stress showed a pattern that was similar to the numerical result. The yield stress obtained from the experimental stress-strain curve of the mild steel ST37 was 344 MPa, i.e. 1.7% lower than from the numerical simulation. The experimental flow stress of the mild steel ST37 also had a similar pattern to the numerical results.

Based on all tests conducted to assess SHPB bar straightness, the experimental results were well aligned with those from the numerical simulation. The difference in yield stress between the experimental and the numerical results in this study were not significant and still acceptable (<5%). The trend of the flow stresses obtained from the experimental results for the aluminum 6061 and the mild steel ST37 were in good agreement with the numerical results.

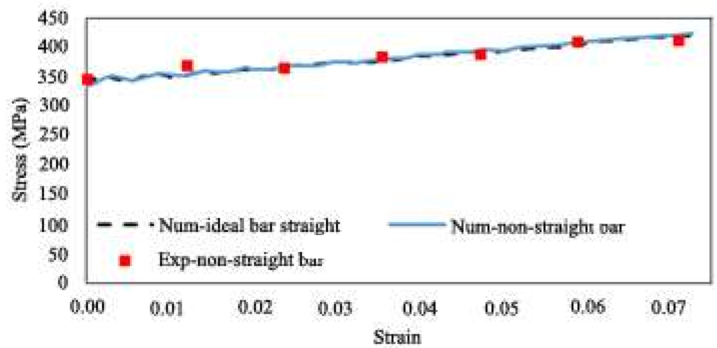

Figure 11 Result comparison between numerical simulation for ideal bar straightness [31], non-straight, and experimental work for non-straight bar.

Furthermore, by referring to the straightness condition of the bars with an average bar straightness deviation of 0.24 mm per 100 mm for the incident bar and 0.36 mm per 100 mm for the transmitter bar, the recommended bar straightness tolerance proposed by Kariem, *et al.* of 0.25 mm per 100 mm can be extended. A comparison between the ideal and non-straight bars validated through the numerical simulation in this work is shown in Figure 11, with an average value of bar straightness of 0.36 mm in the transmitter bar, the stress-strain curve result is still acceptable with a difference of 1.07% between an ideal and a non-straight bar. The extension of the bar straightness value from 0.25 mm to 0.36 mm per 100 mm will make the bar component straightness tolerance more realistic in terms of market availability and manufacturing limitations in developing countries.

5 Conclusion

Experimental and numerical simulation works were conducted to critically evaluate the effects of SHPB straightness. The experimental results showed consistent results in terms of recorded strain rates and stress-strain curves compared to the numerical simulation. The deviation of bar straightness was assessed through combined experiment-validation approaches, which indicated that the straightness deviation observed, as summarized in Table 1, did not significantly affect the performance of the SHPB. Based on the findings of this study, a new refined recommendation for bar straightness tolerance of 0.36 mm per 100 mm is proposed.

Acknowledgements

The authors gratefully acknowledge the financial support from the Ministry of Research and Higher Education, Indonesia, under the PDUPT 2017 scheme. The authors would also like to thank to LSTC for providing the academic license of LS-DYNA.

Nomenclature

c_o	=	elastic wave velocity
L_s	=	specimen length
E	=	modulus of elasticity
$\dot{\varepsilon}$	=	strain rates
ε	=	strain
σ	=	stress
A	=	bar cross section area
A_s	=	specimen cross section area

References

[1] Hopkinson, J., *On The Rupture of Iron Wire by a Blow*, Manchester Lit Phil Soc. Proc., pp. 40-45, 1872.

[2] Hopkinson, J., *Further Experiments on The Rupture of Iron Wire*, Manchester Lit Phil Soc. Proc., pp. 119-121, 1872

[3] Kolsky H., *An Investigation of the Mechanical Properties of Materials at Very High Rates of Loading*, Proc. Phys. Soc. B, **62**, pp. 676-700, 1949.

[4] Korkolis, Y.P., Mitchell, B.R., Locke, M. & Kinsey, B.L., *Plastic Flow and Anisotropy of a Low-carbon Steel over a Range of Strain-rates*, International Journal of Impact Engineering, **121**, pp.157-171, 2018.

[5] Jia, S., Tan, Q., Ye, J., Zhu, Z. & Jiang, Z., *Experiments on Dynamic Mechanical Properties of Austenitic Stainless Steel S30408 and S31608*, Journal of Constructional Steel Reserach, **179**(2), 106556, pp. 1-10, 2021.

[6] Chen, J., Wei, H., Bao, K., Zhang, X., Cao, Y., Peng, Y., Kong, J. & Wang, K., *Dynamic Mechanical Properties of 316L Stainless Steel Fabricated by an Additive Manufacturing Process*, Journal of Materials Research and Technology, **11**, pp. 170-179, 2021.

[7] Sharma, S. & Samal, M.K., *Experimental Investigation of Strain-Rate and Temperature Dependent Mechanical Properties of SA516Gr.70 Steel and*

Development of an Appropriate Material Model, Journal of Materials Engineering and Performance, **30**, pp. 116-130, 2021.

[8] Deshpande, V.S. & Fleck, N.A., *Isotropic Constitutive Models for Metallic Foams*, Journal of The Mechanics and Physics of Solids, **48**, pp. 1253-1283, 2000.

[9] Fila, T., Koudelka, P., Falta, J., Zlamal, P., Rada, V., Adorna, M., Bronder, S. & Jirousek, O., *Dynamic Impact Testing of Cellular Solids and Lattice Structures: Application of Two-sided Direct Impact Hopkinson Bar*, International Journal of Impact Engineering, **148**, 103767, pp. 1-17, 2021.

[10] Irausquin, I., Perez-Castellanos, J.L., Miranda, V. & Teixeira-Dias, F., *Evaluation of the Effect of the Strain Rate on the Compressive Response of a Closed-Cell Aluminium Foam Using the Split Hopkinson Pressure Bar Test*, Materials & Design, **47**, pp. 698-705, 2013.

[11] Deshpande, V.S. & Fleck, N.A., *High Strain Rate Compressive Behaviour of Aluminium Alloy Foams*, Journal of the Mechanics and Physics of Solids, **24**, pp. 277-298, 2000.

[12] Gilat, A., Goldberg, R.K. & Roberts, G.D., *Experimental Study of Strain-Rate Dependent Behavior of Carbon/Epoxy Composite*, Composites Science and Technology, **62**, pp. 1469-1476, 2002.

[13] Alvandi-Tabrizi, Y., Whisler, D.A., Kim, H. & Rabiei, A., *High Strain Rates Behavior of Composite Metal Foam*, Materials Science and Engineering A, **631**, pp. 248-257, 2015.

[14] Rajak, D.K. & Linul, E., *Crushing Response of Composite Metallic Foams: Density and High Strain Rate Effects*, Journal of Alloys and Compounds, **871**, 159614, pp. 1-9, 2021.

[15] Jia, S., Wang, F., Zhou, J., Jiang, Z. & Xu, B., *Study on the Mechanical Performances of Carbon Fiber/Epoxy Composite Material Subjected to Dynamical Compression and High Temperature Loads*, Composites Structures, **258**, 113421, pp. 1-14, 2021.

[16] Akl, W., Aldraihem, O. & Baz, A., *Dynamic Behavior of Polyurea Composites Subjected to High Strain Rate Loading*, Finite Elements in Analysis and Design, **186**, 103501, pp. 1-12, 2021.

[17] Chouhan, H., Bhalla, N.A. & Bhatnagar, N., *High Strain Rate Performance of UHMWPE Composites: Effect of Moisture Ingress and Egres,* Materials Today, **26**, 101709, pp. 1-12, 2021.

[18] Elmahdy, A. & Verleysen, P., *Mechanical Behavior of Basalt and Glass Textile Composites at High Strain Rates: A Comparison*, Polymer Testing, **81**, 106224, pp. 1-13, 2020.

[19] Cady, C.M., Blumenthal, W.R., Gray III, G.T. & Idar, D.J., *Determining the Constitutive Response of Polymeric Materials as a Function of Temperature and Strain Rate*, Journal De Physique IV, **110**, pp. 27-32, 2003.

[20] Fan, J.T., Weerheijm, J. & Sluys, L.J., *High Strain Rate Tensile Mechanical Response of a Polyurethane Elastomeric Material*, Polymer, **65**, pp. 72-80, 2015.

[21] Fan, J.T., Weerheijm, J. & Sluys, L.J., *Dynamic Compressive Mechanical Response of a Soft Polymer Material*, Materials and Design, **79**, pp.73-85, 2015.

[22] Nasraoui, M., Forquin, P., Siad, L. & Rusinek, A., *Influence of Strain Rate, Temperature and Adiabatic Heating on the Mechanical Behaviour of Poly-Methyl-Methacrylate: Experimental and Modelling Analyses*, Materials and Design, **37**, pp. 500-509, 2012.

[23] Li, Z. & Lambros, J., *Strain Rate Effects on the Thermomechanical Behavior of Polymers*, International Journal of Solids and Structures, **38**, pp. 3549-3562, 2001.

[24] Zhou, J., Heisserer, U., Duke, P.W., Curtis, P.T., Morton, J. & Tagarielli, V.L., *The Sensitivity of the Tensile Properties of PMMA, Kevlar and Dyneema to Temperature and Strain Rate*, Polymer, **225**, 123781, pp. 1-11, 2021.

[25] Garcia-Gonzales, D., Rusinek, A., Bendarma, A., Bernier, R., Klosak, M. & Bahi, S., *Material and Structural Behaviour of PMMA from Low Temperatures to Over The Glass Transition: Quasi-Static and Dynamic Loading*, Polymer Testing, **81**, 106263, pp. 1-9, 2020.

[26] Hu, W., Guo, H., Chen, Y., Xie, R., Jing, H. & He, P., *Experimental Investigation and Modeling of the Rate-Dependent Deformation Behavior of PMMA at Different Temperatures*, European Polymer Journal, **85**, pp. 313-323, 2016.

[27] Chen, W. & Ravichandran, G., *Dynamic Compressive Failure of a Glass Ceramic under Lateral Confinement,* Journal of Mechanics and Physics of Solids, **45**, pp. 1303-1328, 1997.

[28] Lee, O.S. & Kim, G.H., *Thickness Effects on Mechanical Behavior of a Composite Material (1001P) and Polycarbonate in Split Hopkinson Pressure Bar Technique*, Journal of Materials Science Letters, **19**, pp. 1805-1808, 2000.

[29] Kariem, M.A., Beynon, J.H. & Ruan, D., *Misalignment Effect in the Split Hopkinson Pressure Bar Technique*, International Journal of Impact Engineering, pp. 60-70, 2012.

[30] Wu, X., Yin, Q., Wei, Y. & Huang, C., *Effect of Imperfect Experimental Conditions On Stress Waves in SHPB Experiments*, Acta Mechanica Sinica, **31**, pp. 827-836, 2015.

[31] Afdhal, Gunawan, L., Dirgantara, T. & Santosa, S.P., *Numerical Simulation for Bar Straightness Effect in SHPB,* Procedia Engineering, Elsevier, **173**, pp. 615-622, 2017.

[32] Song, B., Connelly, K., Korellis, J., Lu, W-Y. & Antoun, B.R., *Improved Kolsky-Bar Design for Mechanical Characterization of Materials Strain Rates*, Meas Sci Technol, **20**, 115701, pp. 1-8, 2009.

[33] Chen, W. & Song, B., *Split Hopkinson (Kolsky) Pressure Bar Design, Testing, and Applications*, Springer New York, London, 2011.

[34] Dunand, M., Gary, G. & Mohr, D., *High Strain Rate Tensile Testing of Sheet Materials Using Three Hopkinson Pressure Bar*, EPJ Web of Conference, **26**, 01010, 1-4, 2012.

[35] Park, C., Huh, H. & Park, J., *Rate-Dependent Hardening Model for Polymer-bonded Explosives with an HTPB Polymer Matrix Considering a Wide Range of Strain Rates*, Journal Composite Materials, **49**(4), pp. 425-438, 2014.

[36] Afdhal, Gunawan, L., Santosa, S.P., Putra, I.S. & Huh, H., *Measurement of Mechanical Properties of ST 37 Material at High Strain Rates Using a Split Hopkinson Pressure Bar*, Applied Mechanics and Material, **660**, pp. 562-566, 2014.

[37] Butt, H.S.U., Xue, P., Jiang, T.Z. & Wang, B., *Parametric Identification for Material of Viscoelastic SHPB from Wave Propagation Data Incorporating Geometrical Effects*, International Journal of Mechanical Sciences, **91**, pp. 46-54, 2014.

[38] Lindholm, U.S., *Some Experiments with the Split Hopkinson Pressure Bar,* Journal of Mechanics Physics of Solids, **12**, pp. 317-335, 1964.

[39] Gama, B.A., *Split Hopkinson Pressure Bar Technique: Experiments, Analyses and Aplication*, Departement of Material Science and Engineering, University of Delaware, Newark, DE, 2004.

[40] Kariem, M.A., Santiago, R.C., Govender, R., Shu, D.W., Ruan, D., Nurick, G., Alves, M., Lu, G. & Langdon, G.S., *Round-Robin Test of Split Hopkinson Pressure Bar*, International Journal of Impact Engineering, **126**, pp. 62-75, 2019.

[41] Gray III, G.T., *Classic Split-Hopkinson Pressure Bar Testing*, ASM Handbook. Mechanical Testing and Evaluation, **8**, pp. 462-476, 2000.